ELSEVIER

Journal of University of Science and Technology Beijing
Volume 15, Number 5, October 2008, Page 611

Materials

Influence of bath composition on the electrodeposition of cobalt-molybdenum amorphous alloy thin films

Qiaoying Zhou, Hongliang Ge, Guoying Wei, and Qiong Wu

College of Science, China Jiliang University, Hangzhou 310018, China
(Received 2007-10-11)

Abstract: Cobalt-molybdenum (Co-Mo) amorphous alloy thin films were deposited on copper substrates by the electrochemical method at pH 4.0. Among the experimental electrodeposition parameters, only the concentration ratio of molybdate to cobalt ions ($[MoO_4^{2-}]/[Co^{2+}]$) was varied to analyze its influence on the mechanism of induced cobalt-molybdenum codeposition. Voltammetry was one of the main techniques, which was used to examine the voltammetric response, revealing that cobalt-molybdenum codeposition depended on the nature of the species in solution. To correlate the type of the film to the electrochemical response, various cobalt-molybdenum alloy thin films obtained from different $[MoO_4^{2-}]/[Co^{2+}]$ solutions were tested. Crack-free homogeneous films could be easily obtained from the low molybdate concentrations ($[MoO_4^{2-}]/[Co^{2+}]\approx0.05$) applying low deposition potentials. Moreover, the content of molybdenum up to 30wt% could be obtained from high molybdate concentration; in this case, the films showed cracks. The formation of these cracked films could be predicted from the observed distortions in the curves of electric current-time (*j*-*t*) deposition transients. The films with amorphous structure were obtained. The hysteresis loops suggested that the easily magnetized axis was parallel to the surface of the films. A saturation magnetization of 137 emu·g^{-1} and a coercivity of 87 Oe of the film were obtained when the deposition potential was –1025 mV, and $[MoO_4^{2-}]/[Co^{2+}]$ was 0.05 in solution, which exhibited a nicer soft-magnetic response.

Key words: Co-Mo alloy; thin films; amorphous; electrodeposition; soft magnetism

1. Introduction

The preparation of magnetic materials of cobalt alloys has received attention since it has wide applications in industry [1-11], mainly in micro-electromechanical systems (MEMS) and magnetic storage devices [12-13]. One of the most interesting applications is the use of the alloy thin films with minimum coercivity and maximum saturation magnetization for magnetic actuation in MEMS. Cobalt forms amorphous alloys with molybdenum; it retains some unusual properties, such as soft magnetism, high corrosion resistance, and high temperature stability [14]. Meanwhile, electrodeposition has proved to be a valid method to prepare magnetic materials [15-20]. Accordingly, the electrodeposition of cobalt-molybdenm amorphous alloy thin films has become a subject of pronounced practical significance. Currently, the influence of electrodeposition conditions on the alloy composition has been studied [21], and certain mechanisms have been proposed for M-Mo systems (M=Co, Fe, Ni) [22]. However, it remains to be established why molybdenum is so strongly favored, as the Mo/Co mass ratio in deposit is higher than the corresponding $[MoO_4^{2-}]/[Co^{2+}]$ in the electrolyte. Moreover, it was that molybdenum incorporation in the cobalt deposit reduced the coercive (H_c) and simultaneously decreased the saturation magnetization (M_s). The aim is to obtain soft cobalt-molybdenum films with the highest possible M_s value.

In this article, several baths containing different $[MoO_4^{2-}]/[Co^{2+}]$ were tested to analyze their influence on the mechanism of induced cobalt-molybdenum codeposition. Furthermore, the possibility of preparing Co-Mo alloy thin films on copper substrates was examined and also the surface topography, structures, and magnetic properties of these films were analyzed, which were used in primary studies for the MEMS development.

Corresponding author: Qiaoying Zhou, **E-mail:** hangzhouzqy@163.com
Also available online at www.sciencedirect.com

2. Experimental procedure

2.1. Materials

The electrodeposition process and film preparation were performed in a conventional three-electrode cell using a microcomputer-controlled ZF-10 potentiostat/galvanostat with the Photoelectric Scanner (PES) software. The solutions contained $CoCl_2 \cdot 6H_2O$, $Na_2MoO_4 \cdot 2H_2O$, $C_6H_{14}N_2O_7$, and Na_2SO_4. All the reagents were of analytical grade. The pH was adjusted to 4.0 by adding 5vol% H_2SO_4. All the solutions were freshly prepared with water, which was distilled twice.

2.2. Methods

(1) Electrochemical testing.

For the electrochemical experiments, the working electrode was a vitreous carbon electrode of 0.0314 cm^2. It was polished using alloy-sand papers of granularity from 10 to 0.1 μm and cleaned ultrasonically for 30 min in acetone before each experiment. The reference electrode was $Hg/Hg_2SO_4/SO_4^{2-}$ mounted in Luggin capillary containing 1 mol/L K_2SO_4 solution. All potentials were referred to this electrode. The counter electrode was a platinum spiral of 40 cm^2. Voltammetric experiments were carried out in quiescent conditions at 10 mV/s, scanning initially towards negative potentials. Only one cycle was run in each voltammetric experiment. Chronoamperometric experiments were performed from an initial potential at which no process occurred to a potential at which reduction occurred.

(2) Preparation of films.

For the preparation of the films, a copper substrate of 4 cm^2 was used. Several baths used in producing Co-Mo alloy films with various molybdenum contents (around 6wt%-30wt%) were developed (Table 1).

Table 1. Electrolyte composition, electrodeposition conditions, and characters of the thin films

No.	Electrolyte	T / °C	pH	Coating
I	0.2 mol/L $C_6H_{14}N_2O_7$+0.32 mol/L Na_2SO_4+0.1 mol/L $CoCl_2$	25	4.0	Smooth bright films
II	0.2 mol/L $C_6H_{14}N_2O_7$+0.32 mol/L Na_2SO_4, $[MoO_4^{2-}]/[Co^{2+}]$=0.05	25	4.0	Coherent smooth films
III	0.2 mol/L $C_6H_{14}N_2O_7$+0.32 mol/L Na_2SO_4, $[MoO_4^{2-}]/[Co^{2+}]$=0.15	25	4.0	Coherent films
IV	0.2 mol/L $C_6H_{14}N_2O_7$+0.32 mol/L Na_2SO_4, $[MoO_4^{2-}]/[Co^{2+}]$=0.3	25	4.0	Cracked films
V	0.2 mol/L $C_6H_{14}N_2O_7$+0.32 mol/L Na_2SO_4, $[MoO_4^{2-}]/[Co^{2+}]$=0.5	25	4.0	Cracked films
VII	0.2 mol/L $C_6H_{14}N_2O_7$+0.32 mol/L Na_2SO_4, $[MoO_4^{2-}]/[Co^{2+}]$=0.8	25	4.0	Cracked broken films

(3) Characterizations of films.

The D/max-rB X-ray diffraction（XRD）structural analysis was performed on a Philips diffractometer. The Cu K_α radiation (λ=0.15406 nm) was selected by means of a diffracted beam flat graphite monochromator. The $2\theta/\theta$ diffractograms were obtained in the range of 10-70° with a step of 0.02° and a measuring time of 15 s per step. The morphology and elemental composition of the films were examined using an X-ray analyzer incorporated in a SIRION-100 field-emission scanning electron microscope (FE-SEM) using standards of pure molybdenum and pure cobalt prior to each quantitative analysis. The magnetic measurements were taken in the Lake Shore 7407 vibrating sample magnetometer (VSM) at room temperature.

The efficiency of deposit preparation was calculated by comparing the deposition charge and chemical analysis of the films.

3. Results and discussion

3.1. Voltammetric study

For the fixed electrodeposition parameters, voltammetric studies from the solutions with variable $[MoO_4^{2-}]/[Co^{2+}]$ were performed (Fig. 1). The results show that a typical nucleation loop is recorded in the reduction zone, revealing that some deposition occurs. During the positive scan, only one oxidation peak around −220 mV is observed (Fig. 1). At a fixed moderate cathodic limit, for $[MoO_4^{2-}]/[Co^{2+}]$ up to 0.05, the oxidation peak appears at more negative potentials than that obtained from the molybdate-free solution (Figs. 1(a)-1(b)). Upon increasing $[MoO_4^{2-}]/[Co^{2+}]$, the peak becomes deformed (Fig. 1(c)-1(e)). Moreover, the voltammetric current appears at less negative potentials when $[MoO_4^{2-}]/[Co^{2+}]$ increases from 0 to 0.3 in solution (Fig. 1(B)), which depends on the different $[MoO_4^{2-}]/[Co^{2+}]$ features in the oxidation.

To confirm the nature of this oxidation peak, the mechanism of the chemical reaction was analyzed. In acidic solutions containing 0.2 mol/L citrate, the electroactive species are CoHCit and $H_rMoO_4Cit^{[r-5]}$ [23]. The reaction proposed for the molybdenum oxide formation from this species is

$$H_rMoO_4Cit^{[r-5]}+(r-5)H^++2e \rightarrow MoO_2+2H_2O+HCit^{2-} \quad (1)$$

According to reaction (1), there is a greater molybdenum oxide current resulted from the higher H^+ concentration. Thereafter, both MoO_2 and CoHCit evolved to the Co-Mo alloy through the formation of an adsorbate intermediate,

$$CoHCit+2e \rightarrow Co+HCit^{2-} \quad (2)$$

$$MoO_2+CoHCit \rightarrow [MoO_2-CoHCit]_{ads} \xrightarrow{Co} Mo \quad [24\text{-}25] \quad (3)$$

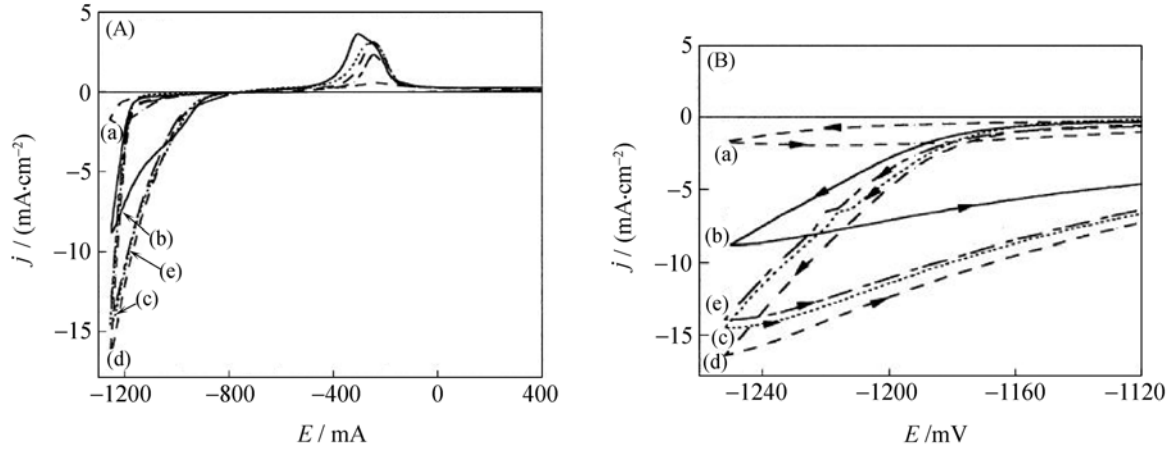

Fig. 1. Cyclic voltammograms (A) and magnified details (B) of the solutions of 0.2 mol/L $C_6H_{14}N_2O_7$+0.32 mol/L Na_2SO_4 and different [MoO_4^{2-}]/[Co^{2+}] (*x*): (a) 0.1 mol/L $CoCl_2$; (b) *x*=0.05; (c) *x*=0.15; (d) *x*=0.3; (e) *x*=0.5.

The results indicate that the presence of a small amount of metallic cobalt (Eq. (2)) is necessary to induce the reduction of the adsorbed intermediate (Eq. (3)). In the first reduction part of these voltammograms, a low current is detected at less negative potentials than –1160 mV. This current, which increases at a higher [MoO_4^{2-}]/[Co^{2+}] is owing to the molybdenum oxide formation [26] before alloy deposition (Figs. 1(a)-1(d)).

However, when [MoO_4^{2-}]/[Co^{2+}] is 0.5, the main voltammetric reduction current is delayed (Fig. 1(e)). Furthermore, when [MoO_4^{2-}]/[Co^{2+}] is 0.8, the shape of the voltammogram changes (Fig. 2), and a quasi-plateau attributed to the formation of molybdenum oxide [26] is recorded. Moreover, the current owing to the Co-Mo deposition is shifted to more negative values. In this case, a smooth band (probably related to hydrogenated species) is recorded, which is followed by a small oxidation peak during the positive scan. Thus, the low [MoO_4^{2-}]/[Co^{2+}] favors alloy deposition, while a higher [MoO_4^{2-}]/[Co^{2+}] leads to the formation of molybdenum oxides, which hinders the Co-Mo deposition.

3.2. Potentiostatic transients

For these solutions, a parallel potentiostatic study was performed under quiescent conditions for a fixed potential but varying [MoO_4^{2-}]/[Co^{2+}]. The results show that an induction time is always observed prior to the appearance of the current, followed by a sharp current increase that attains a quasi stationary value (Fig. 3).

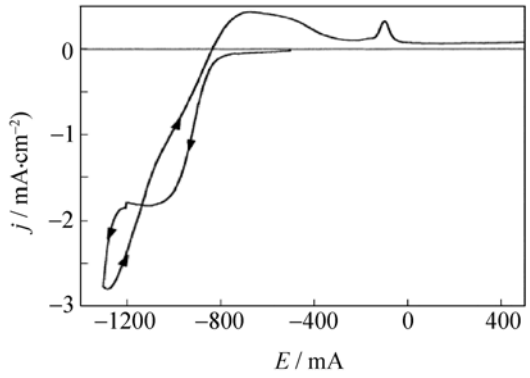

Fig. 2. Cyclic voltammogram of the solution of 0.2 mol/L $C_6H_{14}N_2O_7$+0.32 mol/L Na_2SO_4 and [MoO_4^{2-}]/[Co^{2+}]=0.8.

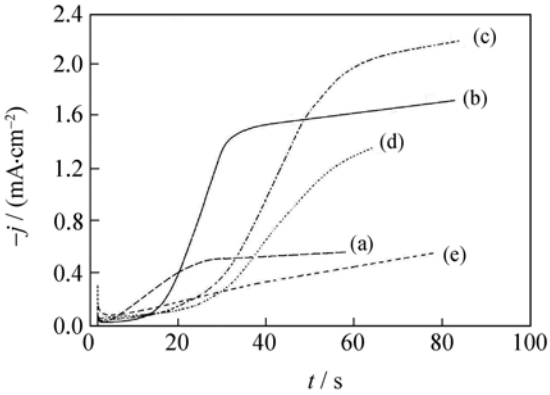

Fig. 3. *j-t* transients recorded from the solution of 0.2 mol/L $C_6H_{14}N_2O_7$+0.32 mol/L Na_2SO_4 and different [MoO_4^{2-}]/[Co^{2+}] (*x*) (starting potential=–650 mV, final potential=–1130 mV): (a) *x*=0; (b) *x*=0.05; (c) *x*=0.15; (d) *x*=0.3; (e) *x*=0.5.

The shape of the *j-t* transient parallels the voltammetric response. The first part is attributed to molybdenum oxide formation and the increase is attributed

to alloy deposition [24]. Corresponding to the molybdenum-free cobalt deposition, a monotonic current increase is observed until a stationary value is attained (Fig. 3(a)). When $[MoO_4^{2-}]/[Co^{2+}]$ is 0.05, it attains similar deposition charges. However, it is necessary to apply lower polarization for the Co-Mo solution than for the cobalt one (Fig. 3(b)). An increase in $[MoO_4^{2-}]/[Co^{2+}]$ up to 0.15 raises both currents (oxide formation and alloy deposition)(Fig. 3(c)). However, when $[MoO_4^{2-}]/[Co^{2+}]$ is above 0.15, the oxide formation current gradually increases and the Co-Mo deposition is progressively delayed (Figs. 3(d)-3(e)). For example, when $[MoO_4^{2-}]/[Co^{2+}]$ is 0.5, the main process does not occur during the experiment (about 300 s) and the deposition does not start until more negative potentials are applied.

When $[MoO_4^{2-}]/[Co^{2+}]$ is higher than 0.5, deformations of the *j-t* transients take place after the nucleation spike and no clear stabilization of the current is observed. Simultaneously, hydrogen evolution is easily detected.

3.3. Compositional, morphological, and structural analysis of Co-Mo alloy thin films

Compositional, morphological, and structural analyses of the Co-Mo alloy thin films obtained from different $[MoO_4^{2-}]/[Co^{2+}]$ and deposition potentials (E(c)) were carried out. The results reveal that the films are composed of Co, Mo, and less O. Moreover, the contents of Mo and O increase with $[MoO_4^{2-}]/[Co^{2+}]$ in solution by applying moderate deposition potentials (Table 2)

Table 2. Connection of deposition potentials and composition of the thin films with bath composition

$[MoO_4^{2-}]/[Co^{2+}]$	E(c) / mV	Co / wt%	Mo / wt%	O / wt%
0.05	−1025	91.91	6.05	2.04
0.15	−1075	80.90	13.45	5.65
0.3	−1130	72.55	19.40	8.05
0.5	−1220	58.09	30.03	11.88

The morphological analysis was performed to detect the content of molybdenum in the films and to correlate the type of the film to the electrochemical response. Fig. 4 shows the FE-SEM micrographs of a pure cobalt film (Fig. 4(a)) and alloy films (molybdenum contents are ranging from 6.05wt% to 30.03wt%) (Figs. 4(b)-4(e)). All the films were obtained under the quiescent conditions. A clear modification in the morphology is observed for the films containing molybdenum, such as, the surface turns dim and presents a nodular morphology whereas a needle like morphology is observed for the pure cobalt film. The analysis of nodular deposits reveals that they are composed of Co+Mo(O). Moreover, the content of molybdenum is a function of both the solution composition and the deposition potential. Thus, the nodular morphology reveals the existence of molybdenum in the films. Similar deposits are obtained using either vitreous carbon or graphite substrates [27].

The content of molybdenum in the films was increased by increasing the $[MoO_4^{2-}]/[Co^{2+}]$ in solution and by applying more negative deposition potentials in a moderate range of potentials. According to other authors [25, 27-28], very negative values of deposition potentials implied the higher molybdenum incorporation in the deposits. Oxygen was detected in the films and its contents increased with $[MoO_4^{2-}]/[Co^{2+}]$ in the solution. It revealed that the Co-Mo alloy thin films of up to 30.03wt% Mo could be obtained from the highest $[MoO_4^{2-}]/[Co^{2+}]$. However, these deposits showed cracks. From the solutions with low $[MoO_4^{2-}]/[Co^{2+}]$ ($\approx$0.05), coherent smooth and crack-free films were obtained with the content of molybdenum lower than 10wt%. Thus, the lowest $[MoO_4^{2-}]/[Co^{2+}]$ are suitable to prepare nicer morphological Co-Mo alloy films.

Structural analysis of the films was performed using XRD. The diffractograms of the Co-Mo alloy films (the molybdenum content is ranging from 6.05wt% to 30.03wt%) show a broad zone centered around 2θ=20° (Fig. 5). These films seem to correspond to a coating with a partially amorphous structure or with a crystalline structure of nanometric crystal size. The former hypothesis is confirmed by an estimation of the crystallite size domain from the peak broadening, using Scherrer's equation [29].

3.4. Magnetic properties of the Co-Mo alloy films

To investigate the magnetic response of the Co-Mo alloy films, the magnetization as a function of the applied magnetic field was performed and compared to the response of a pure cobalt coating.

The strong uniaxial anisotropy was exhibited when the applied field was parallel to the film surface. From the parallel and perpendicular hysteresis loops obtained with the vibrating sample magnetometer (VSM), very different values of the saturation fields (H_s) are observed for parallel ($H_{s//}$=450 Oe) and perpendicular ($H_{s\perp}$>20000 Oe) (Fig. 6). Thus, an easier magnetiza-

tion in the parallel-applied field is observed. Similar magnetic responses are observed for the films originating from different baths (Table 1 III, IV and V).

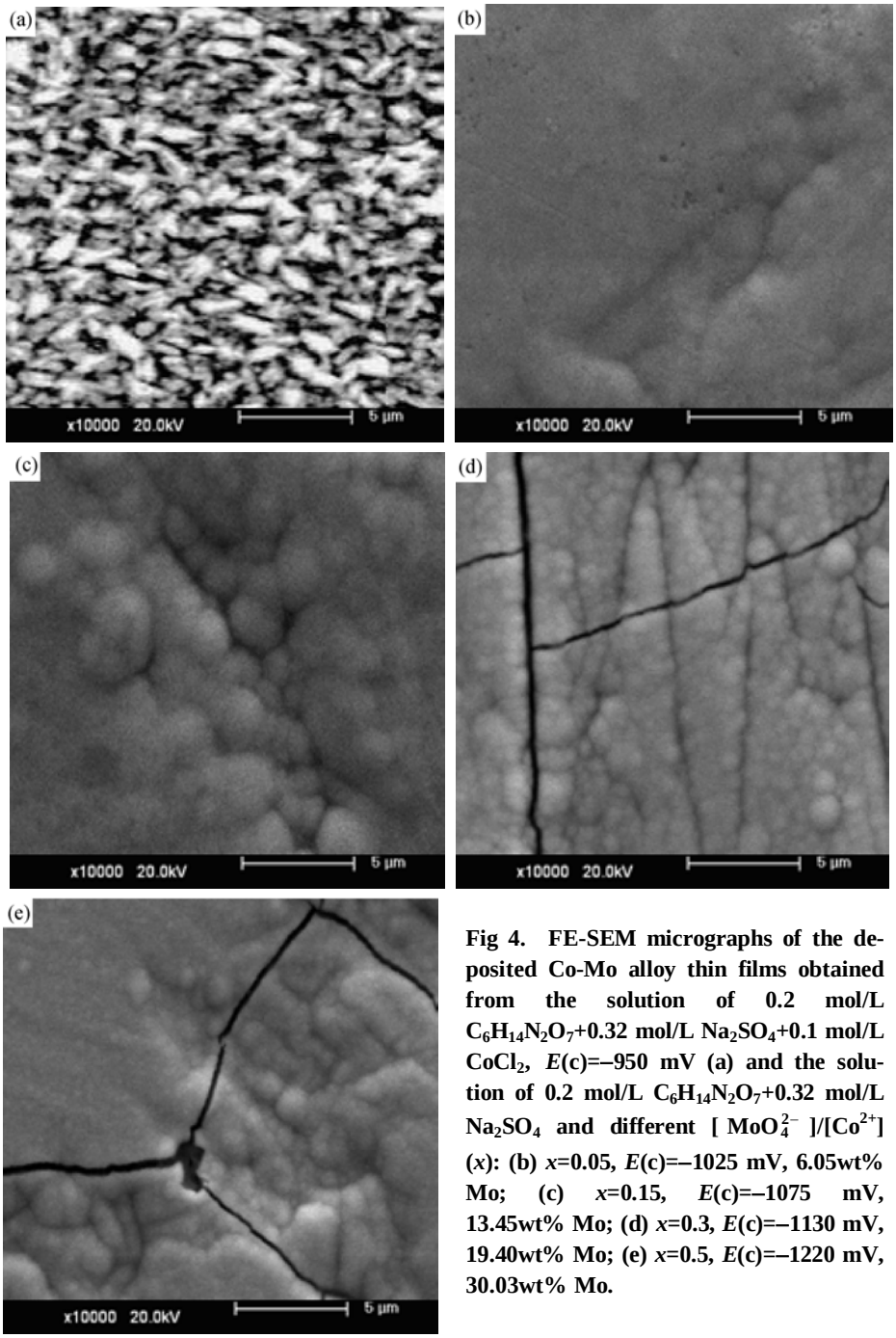

Fig 4. FE-SEM micrographs of the deposited Co-Mo alloy thin films obtained from the solution of 0.2 mol/L $C_6H_{14}N_2O_7$+0.32 mol/L Na_2SO_4+0.1 mol/L $CoCl_2$, *E*(c)=–950 mV (a) and the solution of 0.2 mol/L $C_6H_{14}N_2O_7$+0.32 mol/L Na_2SO_4 and different [MoO_4^{2-}]/[Co^{2+}] (*x*): (b) *x*=0.05, *E*(c)=–1025 mV, 6.05wt% Mo; (c) *x*=0.15, *E*(c)=–1075 mV, 13.45wt% Mo; (d) *x*=0.3, *E*(c)=–1130 mV, 19.40wt% Mo; (e) *x*=0.5, *E*(c)=–1220 mV, 30.03wt% Mo.

The hysteresis loops of the Co-Mo alloy films were measured with VSM. It reveals that the saturation magnetization decreases when the molybdenum content of the films increases from 6.05wt% to 30.03wt%. Simultaneously, a gradually increasing coercivity is observed in the range of 87-109 Oe (Figs. 7(a)-7(d)). For the film of ~6.05wt% Mo, a saturation magnetization (M_s) of about 137 emu·g^{-1} and a coercivity (H_c) of 87 Oe are obtained. The M_s is slightly lower than that of pure-cobalt deposits (M_s=145 emu·g^{-1} [30]). At the same time, H_c is evidently decreased (~160 Oe for deposited cobalt [30]) (Fig. 7(a)). In the previous study, the H_c values of the Co-Mo alloy films (Mo content less than 5wt%) exhibited very close to those of homologous pure-Co deposits, revealing that very low molybdenum contents of the Co-Mo alloy films did not promote the changes in the magnetic response [31]. Low but moderate contents of molybdenum should be more suitable to attain small coercivity values maintaining high saturation magnetization. According to the results obtained from the baths tested, low [MoO_4^{2-}]/[Co^{2+}] clearly leads to the Co-Mo alloy films with good mechanical properties.

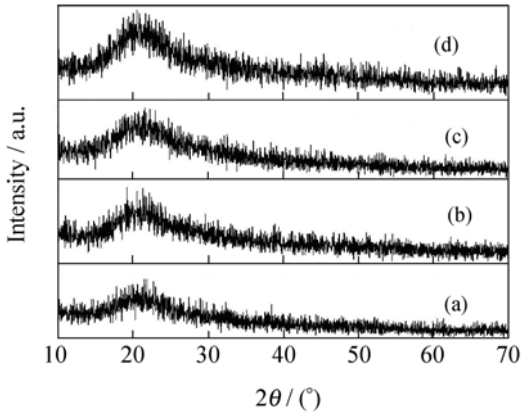

Fig. 5. Diffraction peaks of the deposited Co-Mo alloy thin films obtained from the solutions of 0.2 mol/L $C_6H_{14}N_2O_7$+0.32 mol/L Na_2SO_4 and different $[MoO_4^{2-}]/[Co^{2+}]$ (x): (a) x=0.05; (b) x=0.15; (c) x=0.3; (d) x=0.5.

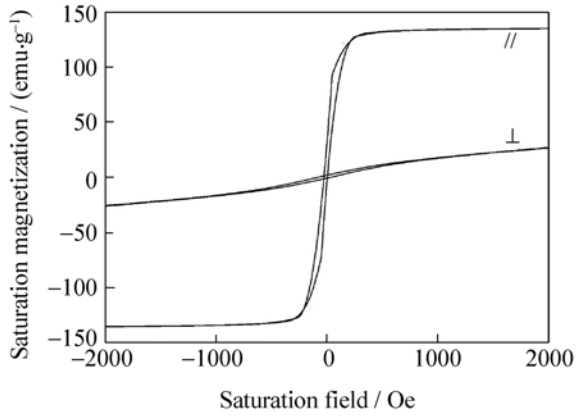

Fig. 6. Zoomed details of the Co-Mo alloy films with parallel and perpendicular hysteresis loops.

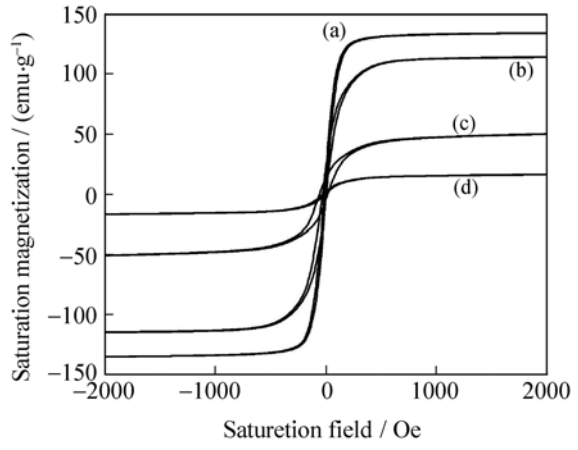

Fig. 7. Zoomed details of parallel hysteresis loops for different Mo contents: (a) 6.05wt%; (b) 13.45wt%; (c) 19.40wt%; (d) 30.03wt%.

4. Conclusions

(1) In the course of Co-Mo codeposition the initial formation is the intermediate molybdenum oxides, whereafter the cobalt nucleation induces the alloy deposition over the oxides.

(2) Co-Mo alloy thin films can be prepared under a moderate potential range. When the deposition potential is below this range, molybdenum oxides form on the electrode, thereby hindering the alloy deposition. Moreover, the current efficiency and the deposit homogeneity considerably diminishes when the deposition potential is higher than the optimum range.

(3) An amorphous structure of the Co-Mo alloy thin films is obtained under these electrodeposition conditions.

(4) The saturation magnetization close to the value exhibited by pure-Co deposits when the molybdenum content is about 6wt%.

References

[1] P.L. Cavallotti, A. Vicenzo, and M. Bestetti, Microelectrodeposition of cobalt and cobalt alloys for magnetic layers, *J. Surf. Coat. Technol*., 76(2003), p.169.

[2] D. Kim, D.Y. Park, B.Y. Yoo, *et al*., Magnetic properties of nanocrystalline iron group thin film alloy electrodeposited from sulfate and chloride baths, *Electrochim. Acta*, 48(2003), p.819.

[3] I. Tabakovic, S. Riemer, V. Inturi, *et al*., Organic additives in the electrochemical preparation of soft magnetic CoNiFe films, *J. Electrochem. Soc*., 147(2000), p.219.

[4] I. Tabakovic, V. Inturi, and S. Riemer, Morphology of soft magnetic CoNiFe films electrodeposited in the presence of saccharin and sodium lauryl sulfate, *J. Electrochem. Soc.*, 149(2002), p.C18.

[5] F.E. Rasmussen, J.T. Ravnkilde, P.T. Tang, *et al.*, [in] *14th European Conference on Solid State Transducers.*, Denmark, 2000, p.915.

[6] T. Osaka, Electrodeposition of highly functional thin films for magnetic recording devices of the next century, *Electrochim. Acta*, 45(2000), p.3311.

[7] Y.K. Kim, H.Y. Son, Y.S. Choi, *et al*., Magnetically soft and electrically resistive CoNiFeS alloy films prepared by electrodeposition, *J. Appl. Phys*., 87(2000), p.5413.

[8] H.S. Nam, T. Yokoshima, T. Nakanishi, *et al*., Microstructure of electroplated soft magnetic CoNiFe thin films, *Thin Solid Films*, 384(2001), p.288.

[9] I. Tabakovic, V. Inturi, and S. Riemer, Composition, structure, stress, and coercivity of electrodeposited soft magnetic CoNiFe films: thickness and substrate dependence, *J. Electrochem. Soc*., 149(2002), p.C18.

[10] G. Shan and J. Nelson, Pulse-reverse electrodeposited nanograinsized CoNiP thin films and microarrays for MEMS actuators, *J. Electrochem. Soc*., 152(2005), p.C190.

[11] E. Gomez and E. Pellicer, Intermediate molybdenum oxides involved in binary and ternary induced electrodeposition, *J. Electroanal. Chem.*, 580(2005), p.222.

[12] M. Duch, J. Esteve, E. Gomez, *et al*., Development and characterization of Co-Ni alloys for microsystems applications, *J. Electrochem. Soc*., 149(2002), p.C201.

[13] M. Duch, J. Esteve, E. Gomez, *et al*., Electrodeposited Co-Ni alloys for MEMS, *J. Micromech. Microeng.*,

12(2002), p.400.

[14] B.X. Liu, W.L. Johnson, and M.A. Nicolet, Structural difference rule for amorphous alloy formation by ion mixing, *J. Appl. Phys*., 42(1983), p.45.

[15] L.T. Romankiw, A path: from electroplating through lithography masks in electronics to LIGA in MEMS, *Eletrochem. Acta*, 42(1997), p.2985.

[16] J. Gobet, F. Cardot, J. Bergquist, *et al*., Electrodeposited cobalt-molybdenum magnetic materials, [in] *Proc. MME'93*, Neuchatel, 1993.p.109.

[17] P.L. Cavallotti, B. Bozzini, L. Nobili, *et al*., Alloy electrodeposition for electronic applications, *Electrochem. Acta*, 39(1994), p.1123.

[18] B. Lochel and A. Maciossek, Electrodeposited magnetic alloys for surface micromachining, *J. Electrochem. Soc*., 143(1996), p.3343.

[19] W.P. Taylor, M. Schneider, H. Baltes, *et al*., [in] *Proc of the International Conference on Solid-State Sensors and Actuators, Transducers'97*, Chicago, 1997, p.1445.

[20] M. Takai, K. Hayashi, M. Aoyagi, *et al*., Electrochemical preparation of soft magnetic CoNiFeS film with high saturation magnetic flux density and high resistivity, *J. Electrochem. Soc*., 144(1997), p.1209.

[21] E. Gomez and E. Pellicer, Developing plating baths for the production of cobalt-molybdenum films, *J. Surf. Coat. Technol*., 197(2005), p.238.

[22] E. Hassaing, K.Vu. Quang, and R. Wiart, The kinetics of the induced codischarge of Mo with Ni in citrate-ammonia electrolytes was investigated by means of polarization and ac impedance measurements, *J. Appl. Electrochem*., 19(1989), p.839.

[23] E.J. Podlaha and D. Landolt, Induced codeposition: II. A mathematical model describing the electrodeposition of Ni-Mo alloys, *J. Electrochem. Soc*., 143(1996), p.893.

[24] E. Gomez, E. Pellicer, and E. Valles, Electrodeposited cobalt-molybdenum magnetic materials, *J. Electroanal. Chem.*, 517(2001), p.109.

[25] E.J. Podlaha and D. Landolt, Induced codeposition: III. Molybdenum alloys with nickel, cobalt and iron, *J. Electrochem. Soc*., 144(1997), p.1672.

[26] E. Gomez, E. Pellicer, and E. Valles, Influence of the bath composition and the pH on the induced cobalt-molybdenum electrodeposition, *J. Electroanal. Chem.*, 556(2003), p.137.

[27] K. Murase, H. Ando, E. Matsubara, *et al*., Determination of Mo(VI) species and composition in Ni-Mo alloy plating baths by Raman spectra factor analysis, *J. Electrochem. Soc*., 147(2000), p.2210.

[28] E.J. Podhala and D. Landolt, Induced codeposition: I. An experimental investigation of Ni-Mo alloys, *J. Electrochem. Soc*., 143(1996), p.885.

[29] G.W. Pei, W.L. Zhong, and S.B. Yue, *X-ray Diffraction of Single Crystal, Polycrystalline and Amorphous Materials*, Shandong University Press, Jinan, 1989, p.446.

[30] E. Gomez, E. Pellicer, and E. Valles, Electrodeposition of soft-magnetic cobalt-molybdenum coatings containing low molybdenum percentages, *J. Electroanal. Chem.*, 568(2004), p.29.

[31] E. Gomez, E. Pellicer, and E. Valles, Microstructures of soft-magnetic cobalt-molybdenum alloy obtained by electrodeposition on seed layer/silicon substrates, *J. Electrochem. Commun.*, 6(2004), p.853.

[32] E. Gomez, E. Pellicer, X. Alcobe, *et al*., Properties of Co-Mo coatings obtained by electrodeposition at pH 6.6, *J. Solid State Electrochem.*, 8(2004), p.497.